International Journal of Applied Chemistry.
ISSN 0973-1792 Volume 13, Number 2 (2017) pp. 333-340

http://www.ripublication.com

Synthesis, Structure and Properties of Nanocrystalline $Nd_2Mo_{2-x}Al_xO_9$ Fast Oxide Conductors

N.Kalaivani[a], M.Rajasekhar[a*] and A.Subramania[b]

[a, a] Advanced Energy Research Lab, PG& Research Department of chemistry, Government Arts College, Dharmapuri-636 705, South India.*
[b] Center for Nanoscience and Technology, Institute Pondicherry University, Pondicherry.

Abstract

$Nd_2Mo_{2-x}Al_xO_9$ ($0 \leq x \leq 0.5$) powders synthesize with use of $Nd(NO_3)_3$, $Al(NO_3)_3$, $(NH4)_6Mo_7O_{24}$, and aspartic acid (fuel) in assisted combustion method and it heat at 550˚C for 6 hours. The thermal decomposition, phase identification, surface morphology and ionic conductivity of the samples are study with TGA/DTA, XRD SEM and four probe D.C. method respectively. The formation of $Nd_2Mo_{2-x}Al_xO_9$ confirm with use of FTIR studies. The weight gain and loss performance confirm with use of thermochemical techniques (TGA/DTA). The nanoparticle size measure with TEM studies. The synthesized materials show the reasonable ionic conductivity. These results indicate the assisted combustion method is a promising method to prepare nanocrystalline $Nd_2Mo_{2-x}Al_xO_9$ for solid oxide fuel cell.

Keywords: Ionic conductivity, Scanning Electron Microscopy**,** Transmission Electron Microscope, Thermal Analysis.

1. INTRODUCTION

Solid oxide fuel cells (SOFCs) which convert chemical energy directly into electrical energy have been viewed as promising new power-generating systems and true multi-fuel energy devices [1]. Recently significant efforts have been directed towards the

development of intermediate temperature solid oxide fuel cell (IT-SOFC) due to its high power density and high working efficiency and its temperature range is 500-800˚C. Mixed ionic-electronic conductivity (MIECs) has attracted attention of researchers due to its high thermal and chemical stability along with high oxygen diffusion and ionic conductivity. (2)

For the fuel cell, Lanthanum Strontium Manganite (LSM) was used as the cathode, YSZ as electrolyte and Ni–YSZ cermet for the anode. It is essential that the chosen interconnect material has the highest chemical stability, the highest oxidation resistance as well as the highest electrical conductivity [3].The permanent increment of human population is accompanied by increase of energy demand and more restrictive environmental regulations. In that instance, the Solid Oxide Fuel Cells (SOFC) technology has emerged as an efficient substitution of the presently existing energy devices [4]. Fuel cells are important class of electrochemical device which converts chemical energy into electrical energy in a clean and calm way. [5].Assisted combustion synthesis (ACS) or self-propagating high-temperature synthesis (SHS) is an effective, low-cost method for production of various industrially useful materials. [6].

The high oxygen ion conductivity over wide range of temperature and oxygen pressure in stabilized zirconia has led to its use as a solid oxide electrolyte which is a variety of electrochemical applications. They have wide range of potential applications whether ranging from providing power for portable devices (eg. Mobile phones, laptop computers) and transport applications, to small and large scale stationary power applications [7].

2. EXPERIMENTAL STUDIES AND CHARACTERIZATION PROCESSES

The nanocrystalline $Nd_2Mo_{2-x}Al_xO_9$ powder was synthesized by assisted combustion method were using high purity $Nd(NO_3)_3$, $(Al(NO_3)_3$, $(NH4)_6Mo_7O_{24}$ and aspartic acid as fuel. All the reagents were purchased from Sigma Aldrich, >99.9%), the required stoichiometric amounts of the starting materials were dissolved in double distilled deionized water in order to obtain a homogeneous solution. This solution was kept at constant heating at 80˚C to obtain the foamy powders of $Nd_2Mo_{2-x}Al_xO_9$. The foamy powder was calcined out in a muffle furnace at 550˚C for 6 hours.

3. STRUCTURAL CHARACTERIZATION ANALYSIS:

X-ray powder diffraction (XRD) data were collected at room temperature with a diffractometer (Model: Philips X˙ Pert MPH^R) with Cu Kα radiation). The datas were recorded in the range of 10-70˚ with a 0.02˚ steps. The particle size and morphology of the produced powder was analysed with a JEOL scanning electron microscopy (SEM) (Model: JSM-840A) equipment with INCA.

The thermal decomposition of the polymeric precursors was characterized by perkin-Elmer TG/DTA thermal analysis (Model; Pyris Diamond). The TGA is a process which relies on measuring the change in physical and chemical properties of a sample as a function of temperature (with constant heating rate) or as a function of time (with constant temperature). It is predominantly used for determining the features of a material that exhibit either mass loss or gain due to decomposition, oxidation or loss of volatiles. Differential thermal analysis is a technique in which the temperature of a sample is compared with that of an inert reference material during the programmed change of temperature.

The particle size of the synthesized powder was observed by means of a JOEL transmission microscope (Model: 1200 EX).The synthesized sample was analysed by FTIR spectrometry. During this process, a small amount of powder was placed at FTIR spectroscopy IR grade which region of about 4000-400cm^{-1}. The ionic conductivity of the sintered pellets were measured by a dc-four probe method which temperatures range 200-700^{0}C in air.

4. RESULT AND DISCUSSION

4.1. Analysis of Crystal Structure

The X-ray powder diffraction (XRD) patterns of $Nd_2Mo_{2-x}Al_xO_9$ is shown in Fig 4.1. In general, all the diffracted peaks were broader than usually observed for highly crystalline powder. The lattice parameter was calculated for the synthesized $Nd_2Mo_{2-x}Al_xO_9$ at 550˚C for 6 hours, it has lattice constant value a = 7.1540(5) A˚ which is good agreement with literature value. Though α-$Nd_2Mo_2O_9$ is assumed to have a monoclinic symmetry, distortion was reported and it was observed under normal x-ray investigation. Moreover, most of the reflections of the α-$Nd_2Mo_2O_9$ phase are comparable to the reflections of the high-temperature cubic β-phase. Hence, the low-temperature α-phase is considered to have a pseudo-cubic symmetry and has been indexed with respect to a cubic symmetry. The XRD patterns of the Al-doped ($x \leq 0.7$) samples appear to be similar to that of the β-$Nd_2Mo_2O_9$ phase. Therefore, the lattice parameters for all compositions were refined on the basis of the cubic symmetry. The variation of the lattice parameters of $Nd_2Mo_{2-x}Al_xO_9$ as a function of Aluminum content is presented in Fig.4.1. As the amount of Al is increased with decrease the lattice parameter, because of the incorporation of a smaller Al^{3+} ion (r = 0.56A°) into a larger Mo^{3+} ax(r = 0.83A˚) lattice site in the $Nd_2Mo_2O_9$.

The broadening in the diffracted peaks is attributed to the superfine crystalline nature of composites. These results are in good agreement with the result of orthorhombic structure. The size of the particles were calculated by Scherer equation and it was 30 nm. All diffracted peaks of the samples can be indicated the orthorhombic structure

without the formation of other impurities. The obtained XRD data were profile fitted with X'pert. High score plus software before indexing.

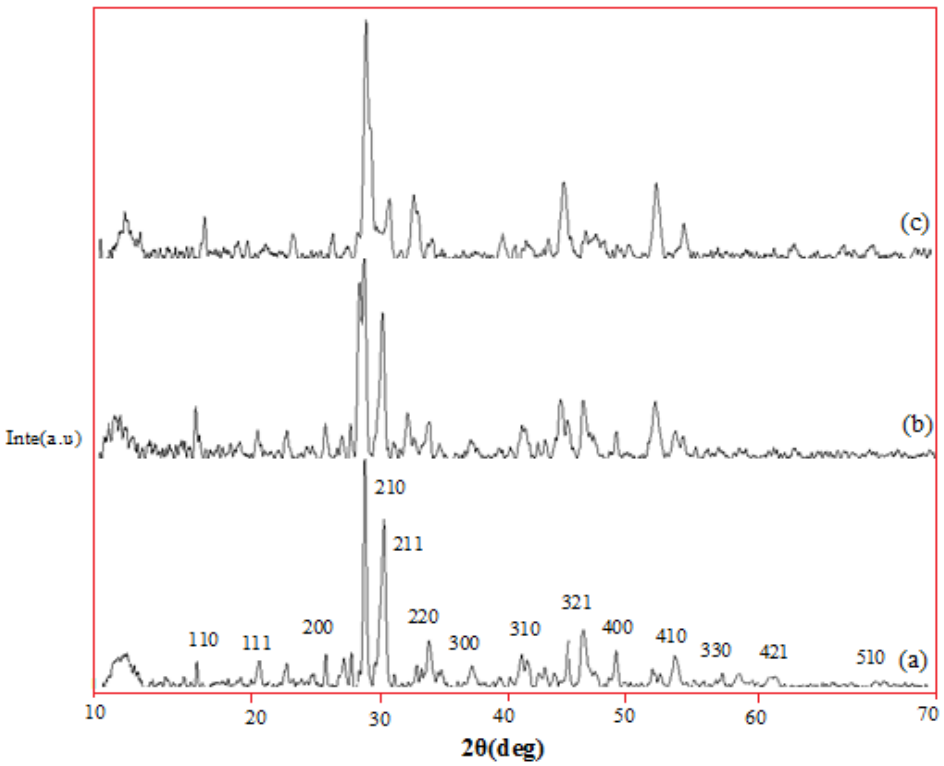

Fig 4.1: X-ray diffraction pattern of $Nd_2Mo_{2-x}Al_xO_9$

4.2. Scanning Electron Microscopy (SEM)

Fig.4.2 shows the SEM microstructure of $Nd_2Mo_{2-x}Al_xO_9$ powder obtained at 550°C for 6 hours. The surface morphology of the synthesized product was good and it has different pores and grains. Further, the SEM image indicated that the particles are agglomeration. All the samples are relatively dense and do not show much difference in density. However Al doping significantly improves the grain growth. The average grain size of the doped samples is in between 4 and 12 μm. The average crystallite size was 30 nm. The particles are uniformly distributed. There is an agglomerate ion of the particles. The particles of the synthesized product are in nanorange.

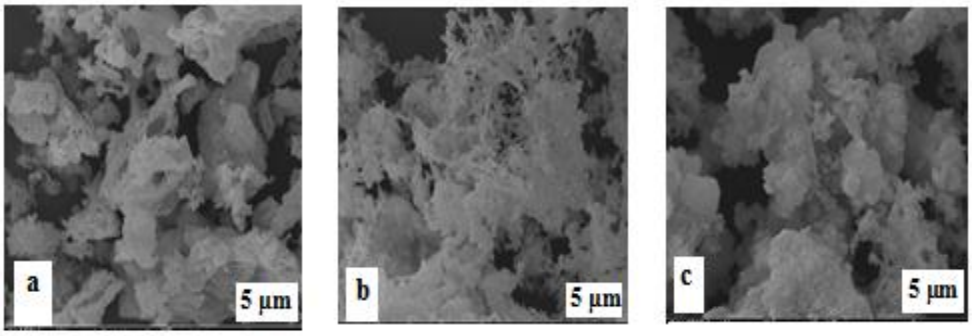

Fig 4.2: SEM photograph of $Nd_2Mo_{2-x}Al_xO_9$

4.3. Thermal Analysis (TGA/DTA)

Fig 4.3.shows that the TGA/DTA pattern obtained on $Nd_2Mo_{2-x}Al_xO_9$ powder. The sample heating from 100˚C-800˚C, it shows slight weight loss of about 0.054mg/min. Again the sample shows a weight increase from 105.3˚C -386.39˚C of 0.167mg/min. The weight gain and weight loss indicated that the $Nd_2Mo_{1.5}Al_{0.5}O_9$ powder exhibited easy reversible absorbtion-desorbtion of oxygen from air. The weight loss is minimum because of the removal of residual H_2O and different gases. The chemical decomposition with an increases of temperature was examined through DTA and it appeared as the endothermic and exothermic peaks in the DTA curve. From the above TGA/DTA data, we know the $Nd_2Mo_{1.5}Al_{0.5}O_9$ gradually absorbs the oxygen from air with temperature.

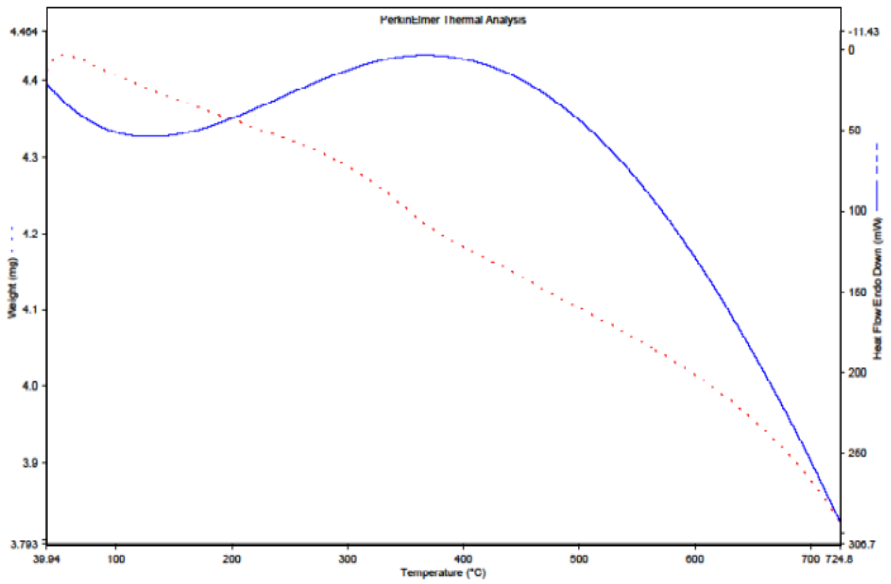

Fig. 4.3: TGA &DTA of $Nd_2Mo_{1.5}Al_{0.5}O_9$

4.4. FTIR Analysis

FTIR spectroscopy was used to confirm verify the functional groups present in the crystal and is investigated their vibrational behavior in solid state of $Nd_2Mo_{1.5}Al_{0.5}O_9$ powder, it was recorded in the range of 4000 cm^{-1} to 400 cm^{-1}. The infrared spectrums of synthesized samples of $Nd_2Mo_{1.5}Al_{0.5}O_9$ powder are shown in fig.4.4. The broad band at 1420.4 cm^{-1} can be assigned to vibration mode of chemically bonded hydroxyl groups. The powder exhibited a strong bond at 500-800 cm^{-1} due to the stretching mode of Mo-O bond in the structure. The peak appeared at 821.1 cm^{-1} corresponds to the H-O-H bond mode confirming the presence of moisture in the sample. The peak appeared at 1420.4 cm^{-1} is due to the presence of CO_2 in the sample. $Nd_2Mo_{1.5}Al_{0.5}O_9$ exhibited a low intensity peak at 754.5 cm^{-1}. The peak appeared at 1354.6 cm^{-1} is related to the O-H stretching vibration of H_2O in the sample. The broad band at 1420.4 cm^{-1} can be assigned to vibration mode of chemically bonded hydroxyl groups.

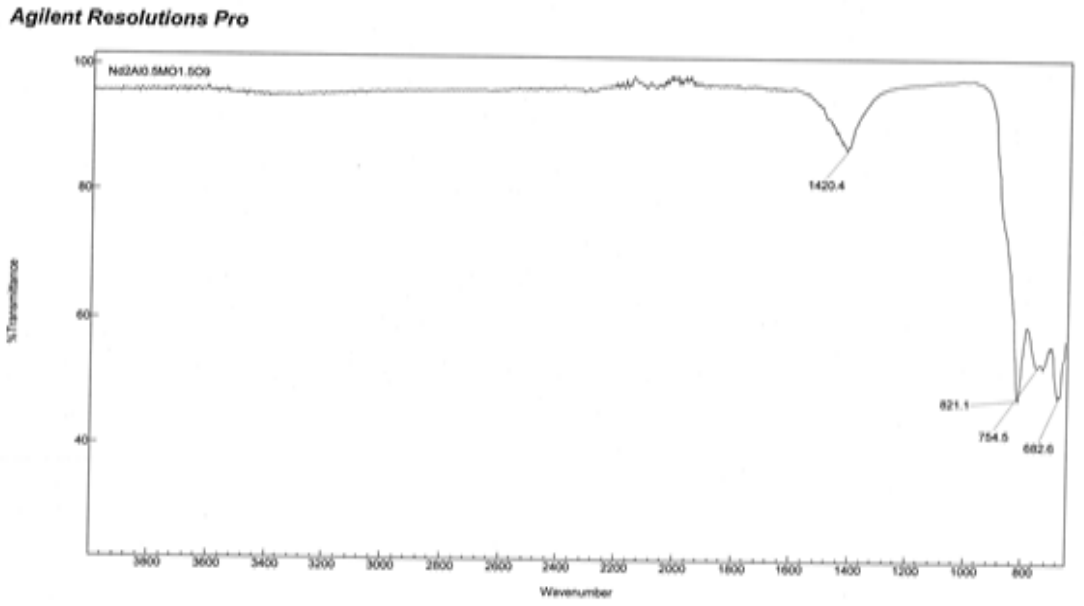

Fig 4.4: FT-IR spectrum of $Nd_2Mo_{1.5}Al_{0.5}O_9$

4.5. Conductivity

Arrhenius plot of conductivity of the $Nd_2Mo_{2-x}Al_xO_9$ samples shown in Fig 4.5. For pure $Nd_2Mo_2O_9$, a dramatic change of conductivity occurs at around 565˚C due to a phase transition. The Al-doped $Nd_2Mo_2O_9$ samples exhibit slightly improved conductivity at lower and higher temperatures. Generally, the higher unit-cell free volume in the oxide ion conductor is easier for the oxygen-ion diffusion. On Al-doping,

the cell parameter is decreased due to the ionic radius of Al^{3+} (r=0.56A˚) is smaller than Mo^{3+} (r=0.83˚). Thus, the substitution of Al greatly increases the free volume and therefore the ionic conductivity of Al-doped samples also increases remarkably. It can also be seen that a sharp conduction increases up to x=0.5 in $Nd_2Mo_{1.5}Al_{0.5}O_9$. The $Nd_2Mo_{1.5}Al_{0.5}O_9$ sample exhibits the conductivity of 0.165 S cm^{-1} at 800˚C, it compared with 0.12 S cm^{-1} for the undoped $Nd_2Mo_2O_9$. This result conforms that Al-doping can improve the oxide ion conductivity of $Nd_2Mo_2O_9$ at low and high temperatures. Moreover, the high purity and phase homogeneity of the present sample could help to improve the conductivity of Al-doped $Nd_2Mo_2O_9$ samples.

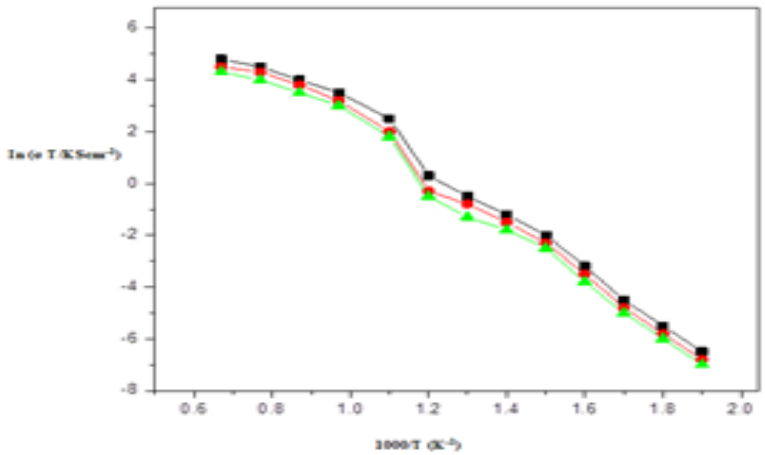

Fig.4.5. Arrhenius plot for overall conductivity for $Nd_2Mo_{1-x}Al_xO_9$ sample

4.6. HRTEM

The transmission electron microscope of the $Nd_2Mo_{1.5}Al_{0.5}O_9$ is shown in Fig.4.5. It can be seen that the synthesized $Nd_2Mo_{1.5}Al_{0.5}O_9$ powder is nanocrystalline in nature and the average particle size was 25 nm. The true size of the sample of prepared $Nd_2Mo_{1.5}Al_{0.5}O_9$ could be determined by TEM investigation.

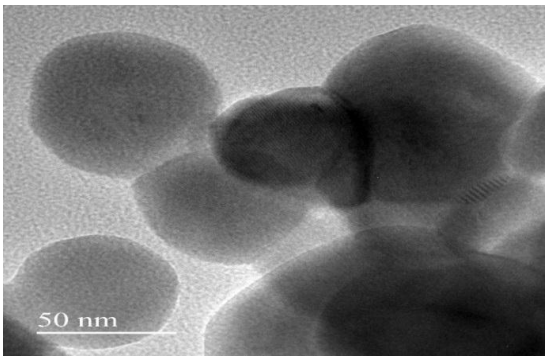

Fig.4.6. Transmission electron micrograph of $Nd_2Mo_{1.5}Al_{0.5}O_9$ nanopowder

5. CONCLUSION

The present investigation was carried out to improve the performance of $Nd_2Mo_{2-x}Al_xO_9$ by the combustion synthesis method. The electrochemical behavior of $Nd_2Mo_{2-x}Al_xO_9$ based material size and sintering temperature. The present work was mainly focused on synthesis, and ionic conductivity of $Nd_2Mo_{2-x}Al_xO_9$.

REFERENCES

[1] A.P. Khandale[a], R.P. Lajurkar[a,b] , S.S.Bhoga[a,*], $Nd_{1.8}Sr_{0.2}Ni_{4-\delta}$:$Ce_{0.9}Gd_{0.9}O_{2-\delta}$ composite cathode for intermediate temperature solid oxide fuel cells, International Journal of Hydrogen Energy 39 (2014) 19039-19050.

[2] A.P.Khandale, S.S.Bhonga* Combistion synthesized $Nd_{2-x}Ce_xCu0_4$ (X= 0-0.25) cathode δmaterials for intermediate temperature solid oxide fuel cell applications, Journal of power sources S195 (2010) 7974-7982.

[3] G. Caboura[a, *], G. Caboche[a], S.Chevalier[a], P. Piccardo[b], Opportunity of metallic interconnects for ITSOFC: Reactivity and electrical prorerty, Journal of power sources 156 (2006) 39-44.

[4] S. Simeonovl, S. Kozhukharov1, J.-C. Grenier2, M. Machkova1, V. Kozhukharov Assessment of Nd**2-xS**rxNiO**4-d** a**s** a Cathodic Material for Solid Oxide Fuel Cell Applications, journal of chemical technology and metallurgy, *48, 1, 2013, 104-110*

[5] Hui S, Roller J, Yick S, Zhang X, Dec`es-Petit C, Xie Y, Maric R, Ghosh D, A brief review of the ionic conductivity enhancement for selected oxide electrolytes, *J. Power Sources* 2007, 172,493-502

[6] Singanahally T. Aruna[a,*] Alexander S. Mukasyan[b,1], Current Option in Solid State and Materials Science, 12 (2008) 44-50.

[7] A. Orera and P.R. Slater[*] New chemical Systems for Solid Oxide Fuel Cells, chem. Mater. 2010, 22, 675-690.

[8] A. Subramania[a,*], T.Saratha[a], S. Muzhumathi[b], Synthesis, Sinterability and ionic conductivity of nanocrystalline Pr-doped $La_2Mo_2O_9$ fast oxide-ion conductors, journal of power sources 167 (2007) 319-324.